数理解析研究所講究録 1249 巻 2002 年 61-71

FRONT DYNAMICS OF THE KPP-FISHER'S EQUATION

M. RODRIGO AND M. MIMURA

ABSTRACT. We study the dynamics of fronts arising in the KPP-Fisher's equation, proposed by Fisher in 1936 to model the propagation of a mutant gene and subsequently studied rigorously in the seminal work of Kolmogorov, Petrovskii, and Piskunov. The approach is via a comparison theorem, where the comparison functions satisfy equations which are linearizable to the heat equation. In some sense, we have obtained a "linearization" of the KPP-Fisher's equation.

Keywords. KPP-Fisher's equation, upper and lower solutions, front dynamics, linearization

1. INTRODUCTION

In this paper, we shall consider the following Cauchy problem for the KPP-Fisher's equation:

$$(1)\qquad \begin{aligned} &u_t = \epsilon^2 \Delta u + f(u), \quad \mathbf{x} \in \mathbb{R}^N \ (N \geq 1), \quad t > 0, \\ &u(\mathbf{x}, 0) = u_0(\mathbf{x}), \quad \mathbf{x} \in \mathbb{R}^N, \end{aligned}$$

where $f \in C^1[0,1]$ satisfies

$$(2)\qquad f(0) = f(1) = 0, \quad f'(0) > 0, \quad f'(1) < 0, \quad f(u) > 0 \quad \text{for} \quad u \in (0,1),$$

and ϵ is any positive real number. This equation arises in several biological models for the propagation of genes and population dynamics (see, for instance, [1], [3], [4], [9], and the references therein).

In the one-dimensional case ($N = 1$), it is well-known that (1) admits a travelling wave front solution (unique up to translation) of the form $u(x,t) = \phi_c(x - ct)$ for every c satisfying $c \geq c^* > 0$. The constant c^* is called the minimal wave speed and ϕ_c is a monotonic decreasing function satisfying

$$\phi_c(-\infty) = 1, \quad \phi_c(+\infty) = 0.$$

The asymptotic behavior of (1) has been well-studied, with special attention being given to finding appropriate initial conditions for which the solution converges to the travelling wave solution ϕ_{c^*} with minimal speed c^* (see [1], [2], [7], [8], [9]). In particular, when the initial function u_0 is a unit step function, Kolmogorov, et. al. [7] showed that the solution of (1) converges in some sense to ϕ_{c^*}. On the other hand, if the initial function has bounded support, then the solution converges to a pair of diverging travelling fronts [9].

Suppose that the initial condition is a pair of travelling fronts moving toward each other. Intuitively, one can expect that the fronts annihilate each other upon collision

M. R. is supported by a Research Fellowship from the Japan Society for the Promotion of Science. M. M. acknowledges the support of Grant-in-Aid for Scientific Research (A) 12304006 and Scientific Research (B) 11214101.

so that the solution tends asymptotically to $u \equiv 1$. The purpose of this paper is to show analytically that this is in fact what happens and, more importantly, to describe the front dynamics of the solution as it evolves in time from the initial condition. We have in mind a general initial condition consisting of an arbitrary number of "peaks" and "valleys".

Especially, when $0 < \epsilon \ll 1$, we can describe the annihilation dynamics quite accurately since (1) can be approximated by a ***nonlinear*** partial differential equation which is ***linearizable*** to the heat equation (see Section 2). Our results are also applicable to higher-dimensional cases ($N \geq 2$). When $N = 2$, for example, we can consider an initial distribution consisting of an arbitrary number of "spots".

The method of proof is by a standard comparison theorem, where the comparison functions satisfy equations which are linearizable to the heat equation. In some sense, we have obtained a "linearization" of the KPP-Fisher's equation since we can describe, in principle, the evolution of the comparison functions for arbitrary initial conditions.

Some works related to ours were done by Hamel and Nadirashvili [5], [6]. They considered time-global solutions ($t \in \mathbb{R}$) of (1) and the mixing of any density of travelling fronts. Our method differs from theirs and the results are obtained for more general initial conditions. In addition, we do not need to assume (as they did) that f is concave in $(0, 1)$.

In Section 2, we construct upper and lower solutions of (1) which satisfy linearizable partial differential equations and then give our main result. In Section 3, we apply this result to the Fisher case $f(u) = u(1-u)$. For various initial distributions, we give some numerical results showing how the comparison functions and the solution of Fisher's equation evolve in time. Finally, in Section 4, we state some current works in progress which generalize our results.

2. Construction of Upper and Lower Solutions of (1) and Statement of Main Result

The derivation of our comparison functions will be done by using some explicit nonlinear transformations. More specifically, suppose that u can be expressed as

$$u = h(v), \tag{3}$$

where v satisfies the linear partial differential equation

$$v_t = \epsilon^2 \Delta v + \alpha v, \quad \alpha \neq 0. \tag{4}$$

We can then compute

$$\begin{aligned} N(u) &\equiv \epsilon^2 \Delta u - u_t + f(u), \\ &= \epsilon^2 (h_v \Delta v + h_{vv} |\nabla v|^2) - h_v v_t + f(h), \\ &= -\alpha v h_v + \epsilon^2 h_{vv} |\nabla v|^2 + f(h). \end{aligned}$$

If we assume further that

$$h_v = \frac{f(h)}{\alpha v}, \tag{5}$$

then we get

$$N(u) = \epsilon^2 h_{vv} |\nabla v|^2 = \epsilon^2 \frac{h_{vv}}{h_v^2} |\nabla u|^2.$$

From (5), we can calculate that

$$\frac{h_{vv}}{h_v^2} = \frac{f'(u) - \alpha}{f(u)}.$$

Therefore, the function u satisfies the equation

$$u_t = \epsilon^2 \Delta u + f(u) - \epsilon^2 \frac{f'(u) - \alpha}{f(u)} |\nabla u|^2, \tag{6}$$

while v satisfies (4), and u and v are related by

$$\int_\nu^u \frac{ds}{f(s)} = \frac{1}{\alpha} \ln v, \quad \nu \in \mathbb{R}, \quad f(\nu) \neq 0. \tag{7}$$

If we can find a solution u of (6) satisfying $N(u) \leq 0$ (resp. $N(u) \geq 0$), then u is an upper (resp. lower) solution of (1).

We now show that upper and lower solutions can be obtained straightforwardly if we assume that f satisfies (2). Letting $\beta \equiv \max_{u \in [0,1]} |f'(u)|$, it follows that

$$-\beta - \alpha \leq f'(u) - \alpha \leq \beta - \alpha$$

for every $u \in (0,1)$.

For an upper solution u^+, we choose $\alpha = \alpha_1 \geq \beta$ so that u^+ satisfies the following:

$$\begin{aligned} & u_t^+ = \epsilon^2 \Delta u^+ + f(u^+) - \epsilon^2 \frac{f'(u^+) - \alpha_1}{f(u^+)} |\nabla u^+|^2, \\ & \int_\nu^{u^+} \frac{ds}{f(s)} = \frac{1}{\alpha_1} \ln v^+, \\ & v_t^+ = \epsilon^2 \Delta v^+ + \alpha_1 v^+. \end{aligned} \tag{8}$$

On the other hand, for a lower solution u^-, we choose $\alpha = \alpha_2 \leq -\beta$ so that u^- satisfies the following:

$$\begin{aligned} & u_t^- = \epsilon^2 \Delta u^- + f(u^-) - \epsilon^2 \frac{f'(u^-) - \alpha_2}{f(u^-)} |\nabla u^-|^2, \\ & \int_\nu^{u^-} \frac{ds}{f(s)} = \frac{1}{\alpha_2} \ln v^-, \\ & v_t^- = \epsilon^2 \Delta v^- + \alpha_2 v^-. \end{aligned} \tag{9}$$

The corresponding initial functions for (8) and (9) will be denoted by u_0^+, v_0^+ and u_0^-, v_0^-, respectively.

We note that (4) can be mapped to the linear heat equation by the transformation $v = \exp(\alpha t) w$ to obtain

$$w_t = \epsilon^2 \Delta w, \quad w_0(\mathbf{x}) = v_0(\mathbf{x}) = \exp\left[\alpha \int_\nu^{u_0(\mathbf{x})} \frac{ds}{f(s)}\right]. \tag{10}$$

The general solution of (10) is given by

$$w(\mathbf{x}, t) = \frac{1}{(4\epsilon^2 \pi t)^{N/2}} \int_{\mathbf{R}^N} G(\mathbf{r}; \mathbf{x}, t) w_0(\mathbf{r})\, d\mathbf{r}, \tag{11}$$

where

$$G(\mathbf{r}; \mathbf{x}, t) = \exp\left(-\frac{|\mathbf{x} - \mathbf{r}|^2}{4\epsilon^2 t}\right), \quad \mathbf{x} = (x_1, x_2, \ldots, x_N)^t, \ \mathbf{r} = (r_1, r_2, \ldots, r_N)^t.$$

Thus, the time-evolutions of $u^{\pm}$ with initial distributions $u_0^{\pm}$ are given by

$$\int_{\nu}^{u^{\pm}(\mathbf{x},t)} \frac{ds}{f(s)} = \tag{12}$$

$$\frac{1}{\alpha_{1,2}} \ln \left[\frac{\exp(\alpha_{1,2}t)}{(4\epsilon^2\pi t)^{N/2}} \int_{\mathbf{R}^N} \exp\left(-\frac{|\mathbf{x}-\mathbf{r}|^2}{4\epsilon^2 t} + \alpha_{1,2} \int_{\nu}^{u_0^{\pm}(\mathbf{r})} \frac{ds}{f(s)} \right) d\mathbf{r} \right].$$

To see how (1) evolves, we choose the initial conditions such that $u_0^-(\mathbf{x}) \le u_0(\mathbf{x}) \le u_0^+(\mathbf{x})$ and substitute in (12).

Now, suppose that $u_0^{\pm}$ are both positive and continuous and satisfy

$$\inf_{\mathbf{x}\in\mathbf{R}^N} u_0^+(\mathbf{x}) > \nu, \quad \inf_{\mathbf{x}\in\mathbf{R}^N} u_0^-(\mathbf{x}) > \nu, \quad (0 < \nu < 1) \tag{13}$$

respectively. Then, it follows that $u_0^+(\mathbf{x}) > \nu$ for every $\mathbf{x} \in \mathbb{R}^N$ and

$$\alpha_1 \int_{\nu}^{u_0^+(\mathbf{r})} \frac{ds}{f(s)} > 0,$$

$$\alpha_1 \int_{\nu}^{u_0^+(\mathbf{r})} \frac{ds}{f(s)} - \frac{|\mathbf{x}-\mathbf{r}|^2}{4\epsilon^2 t} > -\frac{|\mathbf{x}-\mathbf{r}|^2}{4\epsilon^2 t},$$

$$\int_{\mathbf{R}^N} G(\mathbf{r};\mathbf{x},t) v_0^+(\mathbf{r})\, d\mathbf{r} > \int_{\mathbf{R}^N} G(\mathbf{r};\mathbf{x},t)\, d\mathbf{r} = (4\epsilon^2\pi t)^{N/2},$$

$$v^+(\mathbf{x},t) = \frac{\exp(\alpha_1 t)}{(4\epsilon^2\pi t)^{N/2}} \int_{\mathbf{R}^N} G(\mathbf{r};\mathbf{x},t) v_0^+(\mathbf{r})\, d\mathbf{r} > \exp(\alpha_1 t).$$

Therefore, the above statement and the second equation in (8) imply that

$$\lim_{t\to+\infty} v^+(\mathbf{x},t) = +\infty, \quad \lim_{t\to+\infty} u^+(\mathbf{x},t) = 1.$$

In a similar manner, we obtain

$$v^-(\mathbf{x},t) = \frac{\exp(\alpha_2 t)}{(4\epsilon^2\pi t)^{N/2}} \int_{\mathbf{R}^N} G(\mathbf{r};\mathbf{x},t) v_0^-(\mathbf{r})\, d\mathbf{r} < \exp(\alpha_2 t).$$

This statement and the second equation in (9) imply that

$$\lim_{t\to+\infty} v^-(\mathbf{x},t) = 0, \quad \lim_{t\to+\infty} u^-(\mathbf{x},t) = 1.$$

Based on the above results and invoking a comparison theorem for (1) ([1], for instance), we can now state the following

Main Result. *Suppose that u_0^- and u_0^+ are nonconstant continuous functions in $\mathbb{R}^N$ satisfying $0 < u_0^-(\mathbf{x}) \le u_0(\mathbf{x}) \le u_0^+(\mathbf{x}) \le 1$. Then,*

$$u^-(\mathbf{x},t) \le u(\mathbf{x},t) \le u^+(\mathbf{x},t)$$

for every $t \ge 0$, where the dynamics of $u^{\pm}$ are described by (12). *Furthermore,*

$$\lim_{t\to+\infty} u^-(\mathbf{x},t) = \lim_{t\to+\infty} u(\mathbf{x},t) = \lim_{t\to+\infty} u^+(\mathbf{x},t) = 1.$$

In the one-dimensional case, this result implies that if the initial function u_0 consists of an arbitrary number of "peaks" and "valleys" (see Figure 1, where u_0 is any continuous function in the shaded region), then they annihilate each other and the solution eventually approaches the steady state $u \equiv 1$. What we would like to emphasize is that not only do we know the asymptotic behavior of the solution, we can also describe the dynamics of the annihilation process from the dynamics of the upper and lower solutions as described by (12). A similar interpretation can be given for higher-dimensional cases as well.

[— Figure 1 —]

3. Numerical Results and Explicit Approximate Solutions of (1) when $f(u) = u(1-u)$

In this section, we consider Fisher's equation and specify $f(u) = u(1-u)$. From a direct computation, we get $\beta = 1$. Choosing $\alpha_1 = 1$, $\alpha_2 = -1$, and $\nu = 1/2$, we obtain the following upper and lower solutions:

$$\begin{aligned} u_t^+ &= \epsilon^2 \Delta u^+ + u^+(1-u^+) + \frac{2\epsilon^2}{1-u^+}|\nabla u^+|^2, \\ u^+ &= \frac{v^+}{1+v^+}, \quad v_t^+ = \epsilon^2 \Delta v^+ + v^+, \end{aligned} \tag{14}$$

$$\begin{aligned} u_t^- &= \epsilon^2 \Delta u^- + u^-(1-u^-) - \frac{2\epsilon^2}{u^-}|\nabla u^-|^2, \\ u^- &= \frac{1}{1+v^-}, \quad v_t^- = \epsilon^2 \Delta v^- - v^-. \end{aligned} \tag{15}$$

Alternatively, we also have

(16)
$$u^+ = \frac{v^+}{1+v^+}, \quad v^+(\mathbf{x},t) = \frac{\exp(t)}{(4\epsilon^2 \pi t)^{N/2}} \int_{\mathbf{R}^N} \exp\left(-\frac{|\mathbf{x}-\mathbf{r}|^2}{4\epsilon^2 t}\right) \frac{u_0^+(\mathbf{r})}{1-u_0^+(\mathbf{r})}\, d\mathbf{r},$$

(17)
$$u^- = \frac{1}{1+v^-}, \quad v^-(\mathbf{x},t) = \frac{\exp(-t)}{(4\epsilon^2 \pi t)^{N/2}} \int_{\mathbf{R}^N} \exp\left(-\frac{|\mathbf{x}-\mathbf{r}|^2}{4\epsilon^2 t}\right) \frac{1-u_0^-(\mathbf{r})}{u_0^-(\mathbf{r})}\, d\mathbf{r}.$$

For the numerical results, we use (14) and (15), while for the analytical results, we use (16) and (17). In all the numerical computations, we fix the mesh spacings to be $\Delta x = 0.01$, $\Delta t = 0.05$ and impose no-flux boundary conditions on a sufficiently large interval.

Here, we only show some results for the one-dimensional case ($N = 1$). Let the initial conditions be

$$u_0(x) = u_0^+(x) = u_0^-(x) = \frac{1}{1+\exp(b\,x)}, \quad b > 0. \tag{18}$$

Making use of (16) and (17), we get

(19)
$$u^+(x,t) = \frac{1}{1+\exp(b\,x - (1+b^2\epsilon^2)\,t)}, \quad u^-(x,t) = \frac{1}{1+\exp(b\,x - (1-b^2\epsilon^2)\,t)},$$

which are both travelling wave solutions. The wave speeds of u^+ and u^- are given by

$$c_{u^+} = \frac{1+b^2\epsilon^2}{b} \quad \text{and} \quad c_{u^-} = \frac{1-b^2\epsilon^2}{b}, \tag{20}$$

respectively. Note that if $0 < \epsilon \ll 1$, then

$$c_{u^+} \approx c_{u^-} \approx \frac{1}{b} \quad \text{and} \quad u^+ \approx u^- \approx \frac{1}{1+\exp(bx-t)}.$$

For Fisher's equation, it is known that the minimal wave speed is $c_F = 2\epsilon$. It is not difficult to see that $c_{u^+} \geq c_F$. On the other hand, if

$$\epsilon^2 b^2 + 2b\epsilon - 1 \leq 0,$$

then $c_{u^-} \geq c_F$. Assume that b is chosen such that the strict inequality is satisfied. It follows that if the solution of Fisher's equation converges to a travelling wave solution, then the speed will be *greater* than the minimal value c_F. This is in contrast to previous studies done on Fisher's equation where initial conditions are sought for which the solution converges to the wave of minimal speed.

Solving (1), (14), and (15) numerically, we obtain the profiles of u, u^+, and u^- shown in Figure 2, where $\epsilon^2 = 0.03$, $b = 1$, and $c_F = 0.34641016$. From (20), we get $c_{u^+} = 1.03$ and $c_{u^-} = 0.97$.

[— Figure 2 —]

Next, we assume a more complicated initial condition such as

$$u_0(x) = u_0^+(x) = u_0^-(x) = \varphi(x-30) + \varphi(x+30) + \frac{1}{2}\varphi(x) - \frac{1}{4}, \tag{21}$$

where

$$\varphi(x) = \frac{1}{2} - \frac{1}{1+m\cosh(bx)}, \quad b, m > 0.$$

In this case, it is not possible to obtain closed analytic forms from (16) and (17). However, we can integrate (1), (14), and (15) numerically and compare the actual solution with the upper and lower solutions. The results are shown in Figure 3, where $\epsilon^2 = 0.1$, $b = 1$, and $m = 10^{-4}$.

[— Figure 3 —]

Other initial distributions can also be considered and the closeness of the comparison functions and the actual solution of Fisher's equation can be compared.

4. Conclusion

In this paper, we studied the annihilation dynamics for the KPP-Fisher's equation. The method we used is to find "nice" comparison functions which satisfy equations linearizable to the heat equation. Our method can be generalized to other problems, some of which are the following:

(i) dynamics of multi-dimensional fronts of (1) for different boundary conditions;
(ii) extensions to systems of reaction-diffusion equations which satisfy a comparison principle, e.g., a Lotka-Volterra competition-diffusion system;
(iii) free boundary problems for (1) which can be reduced to a two-phase Stefan problem;
(iv) extensions to density-dependent nonlinear diffusion equations;
(v) blowup phenomenon for Fujita-type problems.

These problems are currently under investigation.

References

[1] D. G. Aronson and H. F. Weinberger, Nonlinear diffusion in population genetics, combustion, and nerve propagation, in Partial Differential Equations and Related Topics, *Lecture Notes in Mathematics 446*, Springer-Verlag, New York, 1975.

[2] M. Bramson, Convergence of solutions of the Kolmogorov equation to traveling waves, Mem. Amer. Math. Soc., 44 (1983), No. 285.

[3] P. C. Fife, *Mathematical Aspects of reacting and diffusing systems*, Lect. Notes in Biomathematics, 28, Springer-Verlag, Berlin-New York, 1979.

[4] R. A. Fisher, The wave of advance of an advantageous gene, Ann. Eugen., 7 (1936), pp. 355-369.

[5] F. Hamel and N. Nadirashvili, Entire solutions of the KPP Equation, Comm. Pure Appl. Math., 52 (1999), pp. 1255-1276.

[6] F. Hamel and N. Nadirashvili, Travelling fronts and entire solutions of the Fisher-KPP equation in $\mathbb{R}^N$, preprint.

[7] A. Kolmogorov, I. Petrovskii, and N. Piskunov, Étude de l'équation de la diffusion avec croissance de la quantité de la matieré et son application á un probléme biologique, Moscow Univ. Bull. Math., 1 (1937), pp. 1-25.

[8] H. P. McKean, Application of Brownian motion to the equation of Kolmogorov-Petrovskii-Piskunov, Comm. Pure Appl. Math., 28 (1975), pp. 323-331.

[9] F. Rothe, Convergence to pushed fronts, Rocky Mountain J. Math., 11 (1981), pp. 617-633.

Figure Captions

Fig. 1. Profile of an initial condition of (1)

Fig. 2. Profiles of (1), (14), and (15) with initial conditions (18) for $t = 0, 35$, $\epsilon^2 = 0.03$, and $b = 1$

Fig. 3. Profiles of (1), (14), and (15) with initial conditions (21) for $t = 0, 2.5, 7.5$, $\epsilon^2 = 0.1$, $b = 1$, and $m = 10^{-4}$

Institute for Nonlinear Sciences and Applied Mathematics, Graduate School of Science, Hiroshima University, Higashi-Hiroshima, 739-8526, JAPAN
E-mail address: mrodrigo@math.sci.hiroshima-u.ac.jp

Institute for Nonlinear Sciences and Applied Mathematics, Graduate School of Science, Hiroshima University, Higashi-Hiroshima, 739-8526, JAPAN
E-mail address: mimura@math.sci.hiroshima-u.ac.jp

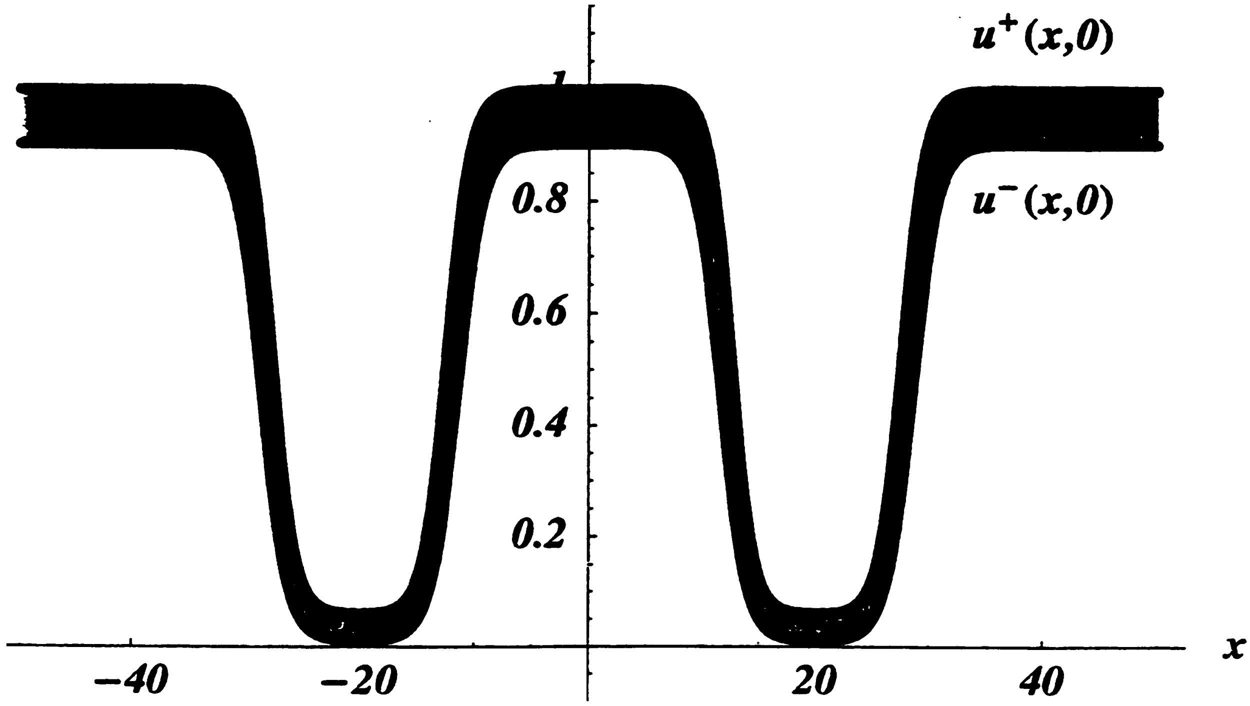

Fig. 1

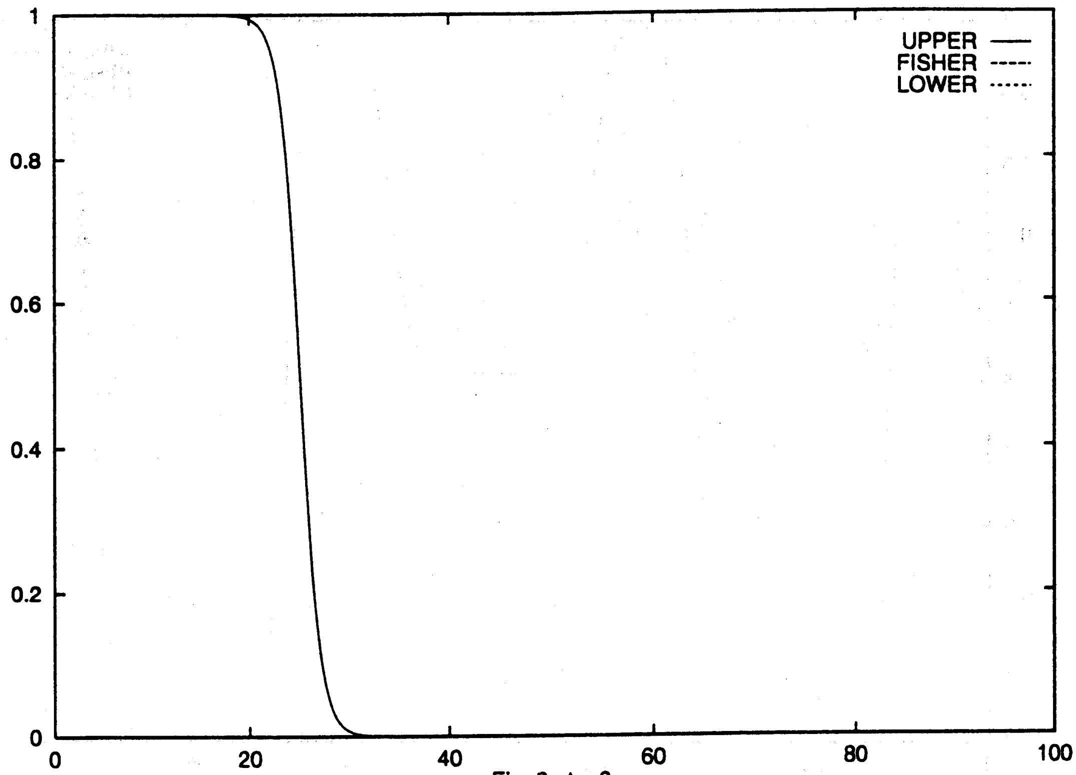

Fig. 2 t = 0

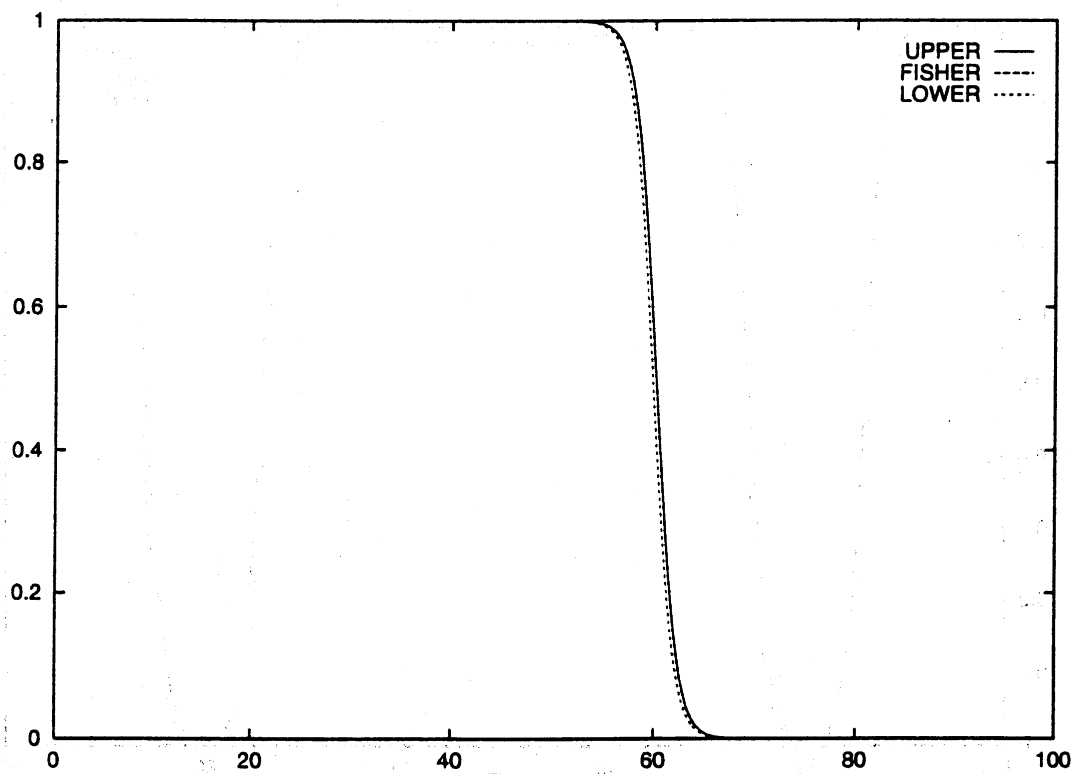

Fig. 2 t = 35

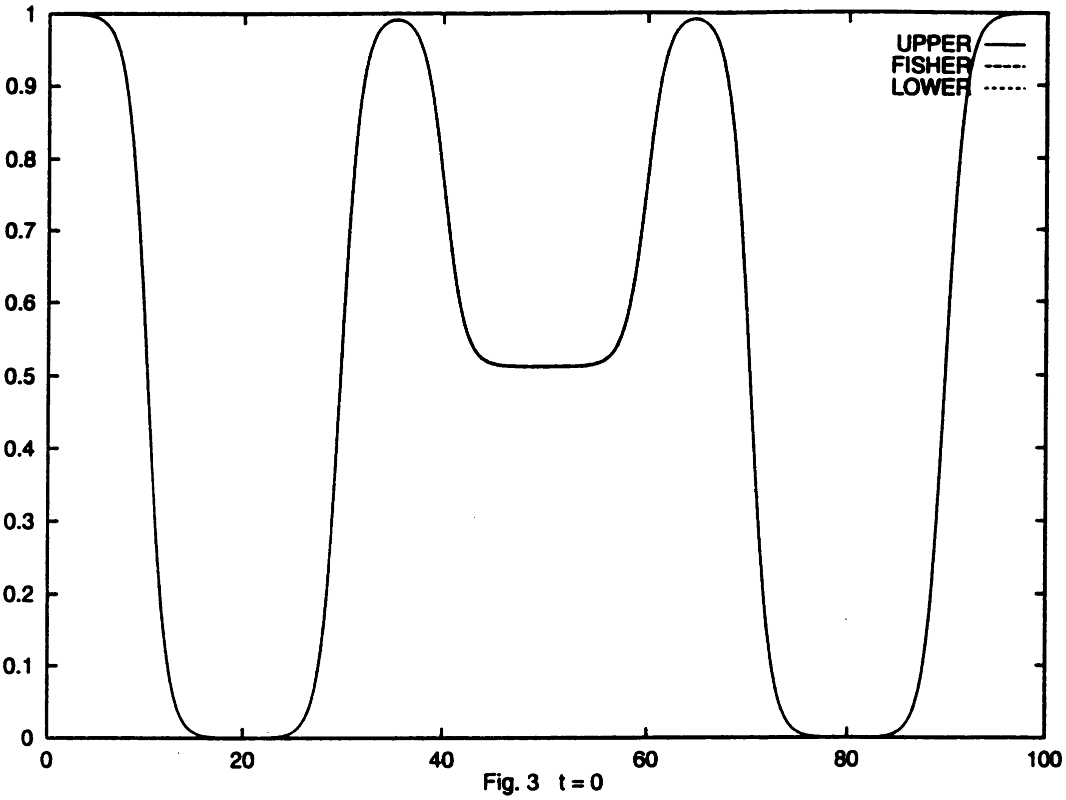

Fig. 3 t = 0

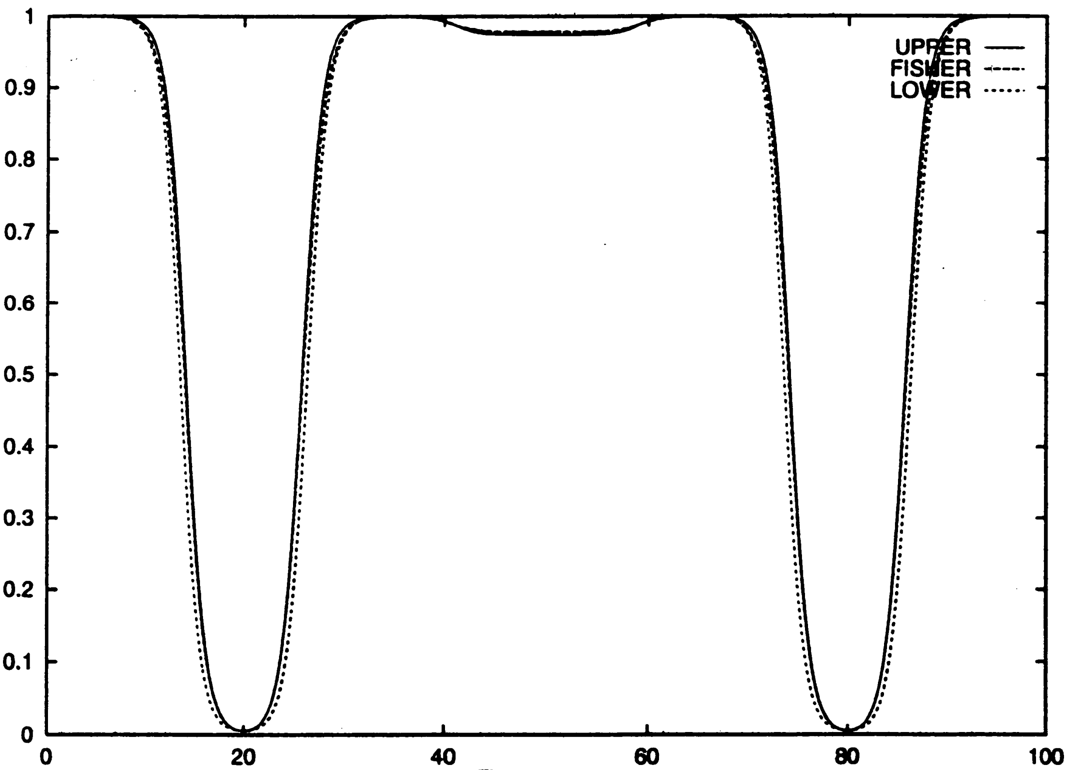

Fig. 3 t = 2.5

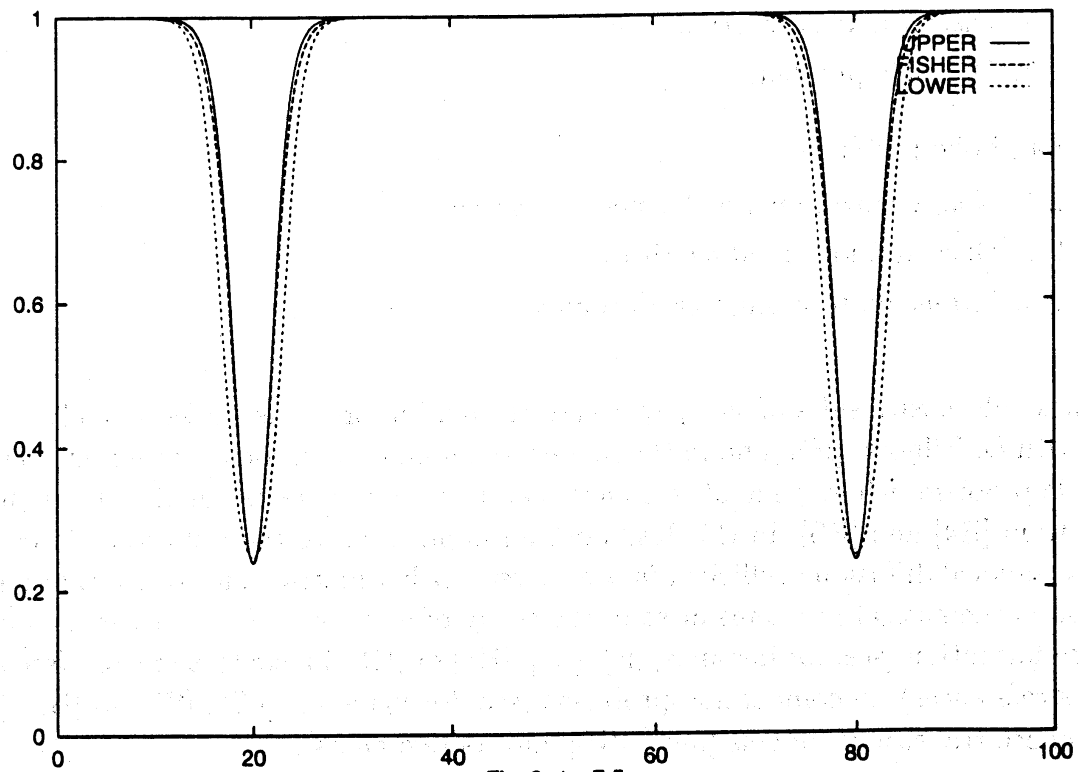

Fig. 3 t = 7.5